Identification of Pathways and Key Genes in Carotid Atherosclerosis by Bioinformatics Analysis

Di Zhang
Jinan University
Bei Jing
Jinan University
Xin Li
Jinan University
Huimei Shi
Jinan University
Shiquan Chang
Jinan University
Zhenni Chen
Jinan University
Yachun Zheng
Jinan University
Yuwei Pan
Tianhe Hospital of Traditional Chinese Medicine
Guoping Zhao (tguo428@jnu.edu.cn)
Jinan University

Research Article

Keywords: carotid atherosclerosis, bioinformatics analysis, inflammation, IL1β

Posted Date: November 30th, 2021

DOI: https://doi.org/10.21203/rs.3.rs-1106491/v1

Abstract

Purpose: Carotid atherosclerosis is a serious vascular disease, leading to various cerebrovascular diseases.

Methods: Gene expression profile of GSE100927 was selected to conduct differentially expressed genes. Then we performed protein-protein interactions, Gene ontology, and Kyoto Encyclopedia of Genes and Genomes analysis. Then we used HUVEC, HAVSMC, and THP-1 induced macrophages cells to conduct experimental verification. The experimental groups were as follows: Control group, Solvent control group, and Palmitic acid group. We measured the levels of reactive oxygen species in three cells via flow cytometer or fluorescence microscope. Then we detected apoptosis of HUVEC cells and HAVSMC cells or observed nucleus of THP-1 induced macrophages cells.

Results: We selected male carotid atherosclerosis, with 10 control samples and 21 atherosclerosis samples. The results of pathway enrichment showed that “Toll-like receptor signaling pathway” ranked first. We chose IL1β, CCL4, SPP1, CCL3, IRF5. MMP7 and MMP9 for experimental verification. Palmitic acid increased the reactive oxygen species levels and the apoptosis rates of HUVEC cells and HAVSMC cells while increasing the activity of THP-1 induced macrophages cells, and it cannot increase the level of reactive oxygen species, and shrink the nucleus. Palmitic acid increased mRNA levels of IL1β, CCL4, SPP1, CCL3, IRF5. MMP7 and MMP9 in HUVEC cells and THP-1 induced macrophages, and increased the mRNA levels of CCL4 and MMP9 in HAVSMC cells not changed the mRNA level of IRF5.

Conclusion: IL1β CCL3, CCL4, SPP1, IRF5, MMP7, and MMP9 are significant markers of carotid atherosclerosis.

1. Introduction

Atherosclerosis, a progressive chronic inflammatory and metabolic disease, features lipid deposition, focal intimal thickening, smooth muscle cell proliferation, and plaque formation[1]. With the improvement of living standards, atherosclerosis and its complications have caused an increase in morbidity and mortality worldwide, accounting for only one third of the death toll in the world[2].

Atherosclerosis of internal carotid artery, resulting in narrowing of the vessel lumen over 50% of the original size, affects nearly 10% of the population over 70 years and causes around 15% of ischemic strokes[3]. It is vital to investigate the underlying mechanism of carotid atherosclerosis. However, atherosclerosis pathogenesis is still not fully clear. Now it is found to participate in lipid metabolism disorders[4], endothelial dysfunction[5], inflammation[6] along with oxidative stress. Therefore, it would be valuable to identify key targets in carotid atherosclerosis. This can help us discover novel chemical composition to treat or prevent carotid atherosclerosis.

In this study, after the detection of expression genes in GSE100927, differentially expressed genes (DEGs) analysis, network analysis, and functional enrichment analysis were conducted, and 7 genes were

screened out. We detected expressions of these genes in HUVEC, HAVSMC, and THP-1 induced macrophages. Interestingly, we found a good correlation among IL1β, CCL3, CCL4, SPP1, IRF5, MMP7, and MMP9.

2. Results

2.1 Genes detected according to the DEG and interaction diagram of proteins

DEG analysis was performed on GSE100927 data set (Figure 1A), and specific DEG results can be seen in the Supplemental Data□Supplementary materials□. The extracted data were normalized and processed by log2 transformation, and a p-value ≤ 0.05 was deemed significant, including 32 upregulated and 13 downregulated genes (Figure 1B). The expression matrices of the identified genes were selected from the GSE100927 and the clustered heat map were constructed with heatmap function (Figure 1C). 45 genes were input into string, we got the protein-protein interaction relationship (Figure 1D). In this part, we got IL1β and MMP9 were key genes.

2.2 Function Enrichment Analysis of DEG

We conducted function enrichment via David. The top 10 significant terms in GO annotation (Figure 2 A, B, C) and 6 significant terms in the pathway enrichment analyses (Figure 1E, Table 2). The results of pathway enrichment showed that “Toll-like receptor signaling pathway” ranked first, and we chose this for experimental verification (Figure 1E). As for GO annotation, we chose the terms ranked first in BP (Biological Process□Table 3), CC (Cellular Component, Table 4), and MF (Molecular Function, Table 5). Venn diagram showed 2 genes (MMP7 and MMP9) were involved in the three terms. Therefore, IL1β, CCL4, SPP1, CCL3, IRF5□MMP7, and MMP9. As for expression levels, IL1β, CCL4, SPP1, CCL3, IRF5□ MMP7, and MMP9 were high expressions in Atherosclerosis group(Figure 2 E-K).

2.3 Palmitic acid affected cell viabilities

To examine the cytotoxicity assay of palmitic acid, HUVEC, HAVSMC, and THP-1 induced macrophages were incubated with different doses of palmitic acid in culture medium containing 10% FBS for 6,12,24,36h. We determined cytotoxicity based on the results of CCK8. 50, 75, 100, 125, 150, 175, and 200 μM palmitic acid lowered the cell viability of HUVEC cells and HAVSMC cells significantly at different time points (Figure 3 A, B, $P < 0.05$), with a maximum response by 200μM, while 100, 125, 150, 175, and 200 μM palmitic acid increased the cell viability of macrophages induced by THP-1 at different time points ($P < 0.05$) with a maximum response by 200μM (Figure 3 C). Given the effects that the incubation of 200μM palmitic acid for 36h decreased cell viability greatly, which caused massive cells death, we considered the incubation of 200μM palmitic acid for 24h might be more suitable.

2.4 Palmitic acid made cells produce ROS

To determine whether the effects of palmitic acid were an intracellular effect, it was investigated whether palmitic acid had effects on the production of reactive oxygen species (ROS) in cells. We examined

intracellular ROS levels in the different groups of cells after palmitic acid incubation for 24 h via fluorescence microscopy and flow cytometry. As shown in Figure 4 A1-A4, palmitic acid incubation increased intracellular ROS levels of HAVSMC cells ($p<0.05$), while the solvent cannot increase those. In Figure 4 B1-B4, palmitic acid incubation increased intracellular ROS levels of HUVEC cells ($p<0.05$), and the solvent cannot increase those. Interestingly, palmitic acid and solvent incubation cannot change the ROS levels of THP-1 induced macrophages (Figure 4 C1-C2).

2.5 The effects of palmitic acid on cells apoptosis

To determine the damaging effects of palmitic acid, it was investigated whether palmitic acid had effects on cell apoptosis and cell nuclear changes. We examined cell apoptosis after palmitic acid incubation for 24 h via fluorescence microscopy and observed nuclear changes via Hoechst 33258. As shown in Figure 5A and 5B, palmitic acid increased the apoptosis proportions of HAVSMC cells ($p<0.05$), while the solvent cannot increase those. In Figure 5C and 5D, palmitic acid increased HUVEC cells apoptosis rate ($p<0.05$), and the solvent cannot increase those. Interestingly, palmitic acid and solvent cannot affect the nucleus of THP-1 induced macrophages(Figure 5E-5F).

2.6 mRNA levels of IL1β, CCL4, SPP1, CCL3, IRF5、MMP7, and MMP9(Figure 6)

We detected mRNA expressions of IL1β, CCL4, SPP1, CCL3, IRF5、MMP7, and MMP9 in HAVSMC cells, HUVEC cells, and THP-1 induced macrophages. Palmitic acid increased the levels of IL1β, CCL4, SPP1, CCL3, IRF5、MMP7, and MMP9 both in THP-1 induced macrophages or HUVEC cells($p<0.05$). Besides, palmitic acid increased the levels of CCL4 and MMP9($p<0.05$), while the expression level of IRF5 has hardly changed.

3. Discussion

Atherosclerosis can occur throughout the arterial vascular system and lead to various diseases. The carotid artery is the most important blood vessel connecting various tissues and organs of the head with the heart, and its importance is self-evident. This study provided evidence that inflammation markers played a major role in atherosclerosis. The palmitic acid model provided new insights into the mechanisms underlying atherosclerosis. The major findings are as follows: (1) Carotid atherosclerosis is closely related to arterial inflammation, including pathway of “Toll-like receptor signaling pathway”, “Cytokine-cytokine receptor interaction”, and “Chemokine signaling pathway”. (2) Macrophages and vascular endothelial cells not vascular smooth muscle cells were involved in vascular inflammation. (3) Palmitic acid causes apoptosis of HUVEC and HAVSMC cells, which indicates that hyperlipidemia can cause blood vessel damage; while it cannot affect THP-induced macrophages. (4) Palmitic acid increased the level of oxidative stress in HUVEC cells and HAVSMC cells, which didn’t increase the level of oxidative stress in THP-induced macrophages.

Oxidative stress played a vital role in the process of the atherosclerotic plaque[7]. Oxidative stress is associated with systemic inflammation, endothelial cell proliferation and apoptosis, and

vasoconstriction, which contribute to endothelial dysfunction, leading to atherosclerosis[8]. Leila[9] considered that cardiovascular diseases, mainly atherosclerosis, can be diagnosed indirectly by measuring oxidative stress markers. Besides, oxidative stress and inflammation are two major proatherogenic factors, responsible for modification of vascular wall integrity[10]. In this study, we found that palmitic acid can induce increased levels of oxidative stress in HUVEC and HAVSMC cells, which is consistent with previous research. Moreover, attenuating oxidative stress potentially slowed the progression of atherosclerotic plaque formation[11]. Chao Ji[12] found that propolis ameliorated restenosis in hypercholesterolemia rabbits with carotid balloon injury by inhibiting lipid accumulation, oxidative stress, and TLR4/NF-κB pathway. Fengwei Zhang[13] found that quercetin was a promising potential in ameliorating atherosclerotic pathophysiology in the rat carotid artery by inhibiting oxidative stress and inflammatory responses mechanistically by modulating the AMPK/SIRT1/NF-κB signaling pathway. The overproduction of reactive oxygen species (ROS) could cause vascular endothelial damage[14-16]. Endothelial dysfunction-induced lipid retention is an early feature of atherosclerotic lesion formation. Apoptosis of vascular smooth muscle cells is one of the major modulating factors of atherogenesis, which accelerates atherosclerosis progression by causing plaque destabilization and rupture. In this study, we found that palmitic acid induces apoptosis of HUVEC cells and HAVSMC cells, which might induce arterial lipid accumulation and exacerbation of the atherosclerosis.

Inflammation is one of major proatherogenic factors, destroying the structure of blood vessels[10]. IL-1 is a critical factor in the process of atherosclerosis. Mice with knockout of ApoE and IL-1β had significantly smaller sizes of atherosclerotic lesions in the aortic sinus and the ratio of atherosclerotic areas of the aorta compared with single ApoE-knockout mice[17]. Moreover, artificial expression of IL-1β on one side of the coronary artery led to increases in the coronary stenosis and aggravation of vascular diseases[18]. In this study, we found that the expressions of IL1β was higher than others in HUVEC cells and THP-1 induced macrophages, which was consistent with the previous conclusions.

The circulating level of the C-C chemokine ligand is increased in atherosclerotic patients[19]. CCL4 can be detected in T-cells, smooth muscle cells, and macrophages in atherosclerotic plaques[20], and further upregulated in vulnerable plaques[21]. In this study, we found that the levels of CCL4 in HAVSMC cells, HUVEC cells, and THP-1 induced macrophages. Ting-Ting Chang[20] considered that the direct inhibition of CCL4 stabilized atheroma and reduced endothelial and macrophage activation. Alexey[22] found that T-cell migration into human atherosclerotic plaques may predominantly occur via CCR5-CCL3 and CX3CR1-CX3CL1 interactions. Ashok[23] considered that the chemokines (family of small cytokines) involved in atherosclerotic plaque formation are CCL3, CXCL4, and macrophage migration-inhibitory factor. Peipei Chen identified four significantly upregulated genes (CCL4, CCL18, MMP9 and SPP1) for diagnosing atherosclerosis. Huan-Lan Bai[24] found that serum levels of SPP1, CD36, ATP6V0D2, CHI3L1, MYH11, and BDNF were differentially expressed in patients with coronary heart disease compared with healthy subjects. We found levels of CCL3 and SPP1in HUVEC cells and THP-1 induced macrophages were higher than those in control group, which was the same as the previous reports.

Interferon regulatory factor 5 (IRF5) played a central role in inflammation, mediating the production of proinflammatory cytokines, such as IL-6, IL-12, IL-23, and TNF-α[25]. Anusha[26, 27] found that IRF5 was detrimental in atherosclerosis, promoting the maintenance of proinflammatory CD11c+ macrophages. John[28] deemed that the positive association of MMP-7 with the calcification of the carotid arteries was revealed. Polonskaya[29] considered that the relative risk of coronary arteries calcification was associated with MMP-9, and MMP-7 level was significantly higher in patients with coronary-heart-disease and verified coronary artery atherosclerosis than in the control group. Our results were the same as those previous reports.

4. Conclusion

Inflammation is closely related to atherosclerosis via bioinformatics and experimental verification. IL1β CCL3, CCL4, SPP1, IRF5, MMP7, and MMP9 are significant markers of carotid atherosclerosis.

5.materials And Methods

5.1 Data sources

The gene expression profile of GSE100927 was downloaded from the Gene Expression Omnibus database (GEO), a publicly accessible online database that facilitates the discovery of genome-wide expression analyses. That dataset is based on the GPL17077 platform (Agilent-039494 SurePrint G3 Human GE v2 8x60K Microarray 039381). The GSE100927 dataset contained 96 samples, including 31 healthy arteries samples and 65 atherosclerotic arteries samples. We selected male carotid atherosclerosis for analysis. And 10 control samples and 21 atherosclerosis samples were found. The raw data were downloaded as MINiML files. The extracted data were normalized and processed by log2 transformation. Fold changes were defined as 2 and a p-value ≤ 0.05 was deemed significant, including 32 upregulated and 13 downregulated genes.

5.2 Functional Annotation for DEGs Using GO, KEGG

The cluster Profiler package is a tool used to implement methods when analyzing and visualizing the functional profiles of genomic coordinates and was used to perform Gene ontology (GO), and Kyoto Encyclopedia of Genes and Genomes (KEGG)[30]. GO analysis is a useful method which includes three key biological aspects: BP (biological process), MF (molecular function), and CC (cellular component)[31]. KEGG is a commonly used bioinformatics database, which analyzes gene functions and enriched genes with their pathways[16, 32]. The GO and KEGG enrichment analyses were performed for DEGs by the cluster Profiler package with the p-value cutoff set to 0.05.

5.3 Constriction of PPI and Venn diagram

String database (https://string-db.org/) is a database containing known and predicted protein-protein interactions (PPI). 45 genes were input into String. We can hide disconnected nodes in the network, and

minimum required interaction score was 0.700. Line thickness indicated the strength of data support. Genes ranked firstly in BP, MF, and CC were input into Venn diagram, and we acquired the same genes.

5.4 Cell lines

T/G HA-VSMCs were purchased from Shenzhen Kuyuan Biotechnology Co., Ltd. (Guangzhou, China). Human umbilical vein endothelial cells (HUVECs) and Tohoku Hospital Pediatrics-1（THP-1,CL-0233) were purchased from Procell Life Science & Technology Co., Ltd. (Wuhan, China). THP-1 cells were cultured with RPMI-1640+10% FBS+0.05mM β-mercaptoethanol (PB180633) +1% antibiotics. HAVSMCs and HUVECs were cultured with 10% FBS+89% DMEM+1% antibiotics at the Formula-Pattern Research Center (School of Traditional Chinese Medicine, Jinan University).

5.5 Reagents

RNAiso Plus was acquired from Takara Biotechnology, Co., Ltd. SYBR®-Green Premix qPCR, an Evo M-MLV RT-PCR kit and RNase-free water (AG11701, AG11602 and AG11012 respectively) were obtained from Accurate Biotechnology Co., Ltd. 2',7'-dichloro-dihydrofluorescein diacetate (DCFH-DA, D6883) and Cell Counting Kit-8 (CCK-8, 96992) was acquired from Sigma-Aldrich (Merck KGaA). Hoechst 33342 (M5112) was obtained from Guangzhou Juyan Biological Co., Ltd. Palmitic acid and solvent （SYSJ-KJ004）were acquired from Xi'an Quantum Technology Development Co., Ltd. Annexin V APC Apoptosis Detection Kit I (62700-80) was purchased from Guangzhou Squirrel Biological Co., Ltd.

5.6 Cell viability and cytotoxicity assays

The viability of cells was determined by the CCK-8 assay. First, all cells were seeded into 96-well plates at a density of $6x10^3$ cells/well for 24 h. To assess the effect of palmitic acid on cells, cells were incubated with palmitic acid at various concentrations (0, 25, 50,75, 100, 125,150, 175 and 200 μM) for 6 h, 12h, 24h, 36h and then subjected to the CCK-8 assay at 37˚C for 1 h. The absorbance (450 nm) was them measured by using a microplate reader (Bio-Tek Instruments, Inc.).

5.7 Experimental grouping

The experimental groups were as follows: Control group, Solvent control group (equal volume solvent), and Palmitic acid group (200 μM Palmitic acid). After co-cultivating with palmitic acid for 24 hours, cells were accepted a series of experiments.

5.8 Intracellular ROS measurement

Cells in 6-well plate or collected in EP tube were incubated at 37˚C for 20 min in PBS containing 20 μM 2',7'-dichloro-dihydrofluorescein diacetate (DCFH-DA). After the DCFH-DA was removed, cells were washed 3 times with PBS. Then intracellular ROS production was measured on an inverted fluorescence microscope or a flow cytometer.

5.9 Cell apoptosis detection via flow cytometry

Annexin V APC and propidium iodide (PI) were used to evaluate the apoptotic rates of cells in different groups. Cells were collected with trypsin and washed with PBS. Subsequently, $1x10^6$ cells were placed in binding buffer and double-stained with Annexin V APC and PI in the dark for 15 min at 4˚C. The proportion of apoptotic cells was then analyzed on a flow cytometer (CytExpert 2.3; Beckman Coulter, Inc.) to determine the apoptotic rate.

5.10 Hoechst 33258 staining

Cells were incubated for 20 min with 5 μL Hoechst 33258 in 0.995 mL PBS. After washing twice with PBS, the fluorescence images were measured on an inverted fluorescence microscope.

5.11 Reverse-transcription quantitative (RT-qPCR)

According to the manufacturer's protocol, total RNA was isolated using RNAiso Plus. Subsequently, cDNA was synthesized based on the instructions of the RT-PCR kit. Then, a Bio-Rad CFX96 Real-Time PCR System (Bio-Rad Laboratories, Inc.) was used to perform qPCR. The amplification parameters were 95˚C for 30 sec, followed by 40 cycles of 95˚C for 5 sec and 60˚C for 34 sec, 95˚C for 15 sec, 60˚C for 60 sec and 95˚C for 15 sec. The relative expression of mRNA was calculated by the $2^{-\Delta\Delta Cq}$ method after normalization to β-actin[15, 33]. For this procedure, SYBR®-Green Premix qPCR and primers (Table 1) were used.

5.12 Statistical analyses

Values are expressed as the mean ± standard deviation. Experiments were repeated three times. GraphPad Prism 8 (GraphPad Software, Inc.) was used to perform statistical analysis. The data were analyzed by one-way ANOVA. Bonferroni's test was the post hoc test after ANOVA. $P<0.05$ was considered to indicate a statistically significant difference.

Abbreviations

Definition	Abbreviation
Biological Process	BP
Cellular Component	CC
C-C Motif Chemokine Ligand 3	CCL3
C-C Motif Chemokine Ligand 4	CCL4
Differentially expressed genes	DGEs
Gene Expression Omnibus	GEO
Gene ontology	GO
Human Aortic Smooth Muscle Cell	HASMC
Human umbilical vein endothelial cell	HUVEC
Interleukin-1β	IL1β
Interferon regulatory factor	IRF5
Kyoto Encyclopedia of Genes and Genomes	KEGG
Molecular Function	MF
Matrix Metallopeptidase 7	MMP7
Matrix Metallopeptidase 9	MMP9
Nuclear factor-k-gene binding	NF-kB
Protein-protein interactions	PPI
Reactive Oxygen Species	ROS
Secreted Phosphoprotein 1	SPP1
Tohoku Hospital Pediatrics-1	THP-1
Toll-like receptor 4	TLR4

Declarations

6. Conflicts of interest

All authors confirm that there are no conflicts of interest related to the content of this article.

7. Funding

The National Natural Science Foundation of China (grant no. 81874404) supported this study.

8. Contributions

Di Zhang, Bei Jing, and Guoping Zhao made considerable contributions to the experimental design, data analysis and experimental procedures. Xin Li, Huimei Shi, Shiquan Chang, Yachun Zheng, Yi Lin, Guoqiang Qian, and Yuwei Pan assisted with English language writing. Guoping Zhao is the corresponding author.

9. Consent for publication

All authors are consent for publication

10. Availability of data and materials

The data used to support the findings of this study are available from the corresponding author upon request. As for GSE100927, it can be acquired from GEO database.

References

[1] KRAAIJENHOF J M, HOVINGH G K, STROES E S G, et al. The iterative lipid impact on inflammation in atherosclerosis [J]. Curr Opin Lipidol, 2021, 32(5): 286-292. doi:10.1097/MOL.0000000000000779.

[2] BARRETT T J. Macrophages in Atherosclerosis Regression [J]. Arterioscler Thromb Vasc Biol, 2020, 40(1): 20-33. doi:10.1161/ATVBAHA.119.312802.

[3] ARBA F, VIT F, NESI M, et al. Carotid revascularization and cognitive impairment: the neglected role of cerebral small vessel disease [J]. Neurol Sci, 2021, doi:10.1007/s10072-021-05629-w.

[4] LEE H, PARK K S, JEON Y J, et al. Lipoprotein(a) and subclinical coronary atherosclerosis in asymptomatic individuals [J]. Atherosclerosis, 2021, doi:10.1016/j.atherosclerosis.2021.09.027.

[5] ARNLOV J, SANG Y, BALLEW S H, et al. Endothelial dysfunction and the risk of heart failure in a community-based study: the Multi-Ethnic Study of Atherosclerosis [J]. ESC Heart Fail, 2020, doi:10.1002/ehf2.13054.

[6] JI E, LEE S. Antibody-Based Therapeutics for Atherosclerosis and Cardiovascular Diseases [J]. Int J Mol Sci, 2021, 22(11): doi:10.3390/ijms22115770.

[7] MURY P, CHIRICO E N, MURA M, et al. Oxidative Stress and Inflammation, Key Targets of Atherosclerotic Plaque Progression and Vulnerability: Potential Impact of Physical Activity [J]. Sports Med, 2018, 48(12): 2725-2741. doi:10.1007/s40279-018-0996-z.

[8] MONTEZANO A C, TOUYZ R M. Reactive oxygen species and endothelial function–role of nitric oxide synthase uncoupling and Nox family nicotinamide adenine dinucleotide phosphate oxidases [J]. Basic

Clin Pharmacol Toxicol, 2012, 110(1): 87-94. doi:10.1111/j.1742-7843.2011.00785.x.

[9] TOUALBI L A, ADNANE M, ABDERREZAK K, et al. Oxidative stress accelerates the carotid atherosclerosis process in patients with chronic kidney disease [J]. Arch Med Sci Atheroscler Dis, 2020, 5(e245-e254. doi:10.5114/amsad.2020.98945.

[10] GRYSZCZYNSKA B, FORMANOWICZ D, BUDZYN M, et al. Advanced Oxidation Protein Products and Carbonylated Proteins as Biomarkers of Oxidative Stress in Selected Atherosclerosis-Mediated Diseases [J]. Biomed Res Int, 2017, 2017(4975264. doi:10.1155/2017/4975264.

[11] HE F, LI J, LIU Z, et al. Redox Mechanism of Reactive Oxygen Species in Exercise [J]. Front Physiol, 2016, 7(486. doi:10.3389/fphys.2016.00486.

[12] JI C, PAN Y, XU S, et al. Propolis ameliorates restenosis in hypercholesterolemia rabbits with carotid balloon injury by inhibiting lipid accumulation, oxidative stress, and TLR4/NF-kappaB pathway [J]. J Food Biochem, 2021, 45(4): e13577. doi:10.1111/jfbc.13577.

[13] ZHANG F, FENG J, ZHANG J, et al. Quercetin modulates AMPK/SIRT1/NF-kappaB signaling to inhibit inflammatory/oxidative stress responses in diabetic high fat diet-induced atherosclerosis in the rat carotid artery [J]. Exp Ther Med, 2020, 20(6): 280. doi:10.3892/etm.2020.9410.

[14] LI J M, SHAH A M. Endothelial cell superoxide generation: regulation and relevance for cardiovascular pathophysiology [J]. American Journal of Physiology-Regulatory Integrative and Comparative Physiology, 2004, 287(5): R1014-R1030. doi:10.1152/ajpregu.00124.2004.

[15] ZHANG D, SUN J X, CHANG S Q, et al. Protective effect of 18 beta-glycyrrhetinic acid against H2O2-induced injury in Schwann cells based on network pharmacology and experimental validation [J]. Experimental and Therapeutic Medicine, 2021, 22(5): doi:ARTN 1241

10.3892/etm.2021.10676.

[16] ZHANG D, YANG B, CHANG S Q, et al. Protective effect of paeoniflorin on H2O2 induced Schwann cells injury based on network pharmacology and experimental validation [J]. Chinese Journal of Natural Medicines, 2021, 19(2): 90-99. doi:10.1016/S1875-5364(21)60010-9.

[17] KIRII H, NIWA T, YAMADA Y, et al. Lack of interleukin-1beta decreases the severity of atherosclerosis in ApoE-deficient mice [J]. Arterioscler Thromb Vasc Biol, 2003, 23(4): 656-60. doi:10.1161/01.ATV.0000064374.15232.C3.

[18] SHIMOKAWA H, ITO A, FUKUMOTO Y, et al. Chronic treatment with interleukin-1 beta induces coronary intimal lesions and vasospastic responses in pigs in vivo. The role of platelet-derived growth factor [J]. J Clin Invest, 1996, 97(3): 769-76. doi:10.1172/JCI118476.

[19] CAGNIN S, BISCUOLA M, PATUZZO C, et al. Reconstruction and functional analysis of altered molecular pathways in human atherosclerotic arteries [J]. BMC Genomics, 2009, 10(13. doi:10.1186/1471-2164-10-13.

[20] CHANG T T, YANG H Y, CHEN C, et al. CCL4 Inhibition in Atherosclerosis: Effects on Plaque Stability, Endothelial Cell Adhesiveness, and Macrophages Activation [J]. Int J Mol Sci, 2020, 21(18): doi:10.3390/ijms21186567.

[21] MONTECUCCO F, LENGLET S, GAYET-AGERON A, et al. Systemic and intraplaque mediators of inflammation are increased in patients symptomatic for ischemic stroke [J]. Stroke, 2010, 41(7): 1394-404. doi:10.1161/STROKEAHA.110.578369.

[22] KOMISSAROV A, POTASHNIKOVA D, FREEMAN M L, et al. Driving T cells to human atherosclerotic plaques: CCL3/CCR5 and CX3CL1/CX3CR1 migration axes [J]. Eur J Immunol, 2021, 51(7): 1857-1859. doi:10.1002/eji.202049004.

[23] MUNJAL A, KHANDIA R. Atherosclerosis: orchestrating cells and biomolecules involved in its activation and inhibition [J]. Adv Protein Chem Struct Biol, 2020, 120(85-122. doi:10.1016/bs.apcsb.2019.11.002.

[24] BAI H L, LU Z F, ZHAO J J, et al. Microarray profiling analysis and validation of novel long noncoding RNAs and mRNAs as potential biomarkers and their functions in atherosclerosis [J]. Physiological Genomics, 2019, 51(12): 644-656. doi:10.1152/physiolgenomics.00077.2019.

[25] KRAUSGRUBER T, BLAZEK K, SMALLIE T, et al. IRF5 promotes inflammatory macrophage polarization and TH1-TH17 responses [J]. Nat Immunol, 2011, 12(3): 231-8. doi:10.1038/ni.1990.

[26] SENEVIRATNE A N, EDSFELDT A, COLE J E, et al. Interferon Regulatory Factor 5 Controls Necrotic Core Formation in Atherosclerotic Lesions by Impairing Efferocytosis [J]. Circulation, 2017, 136(12): 1140-1154. doi:10.1161/CIRCULATIONAHA.117.027844.

[27] POSADAS-SANCHEZ R, CARDOSO-SALDANA G, FRAGOSO J M, et al. Interferon Regulatory Factor 5 (IRF5) Gene Haplotypes Are Associated with Premature Coronary Artery Disease. Association of the IRF5 Polymorphisms with Cardiometabolic Parameters. The Genetics of Atherosclerotic Disease (GEA) Mexican Study [J]. Biomolecules, 2021, 11(3): doi:10.3390/biom11030443.

[28] GAUBATZ J W, BALLANTYNE C M, WASSERMAN B A, et al. Association of circulating matrix metalloproteinases with carotid artery characteristics: the Atherosclerosis Risk in Communities Carotid MRI Study [J]. Arterioscler Thromb Vasc Biol, 2010, 30(5): 1034-42. doi:10.1161/ATVBAHA.109.195370.

[29] POLONSKAYA Y V, KASHTANOVA E V, MURASHOV I S, et al. Association of Matrix Metalloproteinases with Coronary Artery Calcification in Patients with CHD [J]. J Pers Med, 2021, 11(6): doi:10.3390/jpm11060506.

[30] YU G C, WANG L G, HAN Y Y, et al. clusterProfiler: an R Package for Comparing Biological Themes Among Gene Clusters [J]. Omics-a Journal of Integrative Biology, 2012, 16(5): 284-287. doi:10.1089/omi.2011.0118.

[31] GENE ONTOLOGY C. The Gene Ontology (GO) project in 2006 [J]. Nucleic Acids Res, 2006, 34(Database issue): D322-6. doi:10.1093/nar/gkj021.

[32] ALTERMANN E, KLAENHAMMER T R. PathwayVoyager: pathway mapping using the Kyoto Encyclopedia of Genes and Genomes (KEGG) database [J]. Bmc Genomics, 2005, 6(doi:Artn 60

10.1186/1471-2164-6-60.

[33] LIVAK K J, SCHMITTGEN T D. Analysis of relative gene expression data using real-time quantitative PCR and the 2(T)(-Delta Delta C) method [J]. Methods, 2001, 25(4): 402-408. doi:10.1006/meth.2001.1262.

Tables

Table 1 Primer sequences used for PCR

Gene	Forward primer (5'-3')	Reverse primer (5'-3')
IL1β	ATGATGGCTTATTACAGTGGCAA	GTCGGAGATTCGTAGCTGGA
CCL3	AGTTCTCTGCATCACTTGCTG	CGGCTTCGCTTGGTTAGGAA
CCL4	TCGCAACTTTGTGGTAGA	TTCAGTTCCAGGTCATACAC
IRF5	GGGCTTCAATGGGTCAACG	GCCTTCGGTGTATTTCCCTG
MMP7	GAGTGAGCTACAGTGGGAACA	CTATGACGCGGGAGTTTAACAT
MMP9	GGGACGCAGACATCGTCATC	TCGTCATCGTCGAAATGGGC
SPP1	GAAGTTTCGCAGACCTGACAT	GTATGCACCATTCAACTCCTCG

Table 2 KEGG Pathway Enrichments

Term	Pathway	PValue	Genes
hsa04620	Toll-like receptor signaling pathway	0.0004	IL1B, CCL4, SPP1, CCL3, IRF5
hsa04060	Cytokine-cytokine receptor interaction	0.0013	CX3CR1, IL1B, CCL4, CCL3, CCL18, CXCL14
hsa05323	Rheumatoid arthritis	0.0034	MMP1, IL1B, CCL3, ACP5
hsa04062	Chemokine signaling pathway	0.0036	CX3CR1, CCL4, CCL3, CCL18, CXCL14
hsa04380	Osteoclast differentiation	0.0102	FCGR3A, IL1B, ACP5, TREM2
hsa05132	Salmonella infection	0.0334	IL1B, CCL4, CCL3

Table 3 GO annotation （Biological Process）

Term	Pathway	PValue	Genes
GO:0022617	extracellular matrix disassembly	3.24073E-08	MMP12, MMP7, MMP1, SPP1, ADAM8, CAPG, MMP9
GO:0070374	positive regulation of ERK1 and ERK2 cascade	4.51858E-06	HAND2, PLA2G2A, CCL4, CCL3, CHI3L1, TREM2, CCL18
GO:0071356	cellular response to tumor necrosis factor	7.71998E-06	SFRP1, CCL4, CCL3, CHI3L1, CCL18, HAMP
GO:0006955	immune response	8.16275E-06	IL1RN, FCGR3A, IL1B, AQP9, CCL4, CCL3, CCL18, HAMP, CXCL14
GO:0071347	cellular response to interleukin-1	2.90881E-05	SFRP1, CCL4, CCL3, CHI3L1, CCL18
GO:2000503	positive regulation of natural killer cell chemotaxis	0.00012724	CCL4, CCL3, CXCL14
GO:0001649	osteoblast differentiation	0.000129681	SFRP1, IBSP, MYOC, SPP1, CCL3
GO:0006954	inflammatory response	0.00033532	IL1B, CCL4, SPP1, CCL3, CHI3L1, ADAM8, CCL18
GO:0007267	cell-cell signaling	0.000409983	IL1B, CCL4, CCL3, ADRA2C, CCL18, CXCL14
GO:0045780	positive regulation of bone resorption	0.000468124	CA2, SPP1, ADAM8

Table 4 GO annotation （Cellular Component）

Term	Pathway	PValue	Genes
GO:0005615	extracellular space	1.0927E-11	IL1RN, SPON1, MMP7, MYOC, PLA2G2A, HP, CXCL14, MMP9, SFRP1, IBSP, CA2, IL1B, CCL4, SPP1, CCL3, HMOX1, CHI3L1, APOD, CCL18, SCRG1, HAMP
GO:0005576	extracellular region	1.64812E-08	MMP7, MMP1, PLA2G2A, HP, HBA2, TREM2, CXCL14, MMP9, MMP12, IL4I1, SFRP1, IBSP, IL1B, CCL4, APOC1, SPP1, CCL3, APOD, HAMP
GO:0005578	proteinaceous extracellular matrix	2.65218E-07	MMP12, SPON1, SFRP1, MMP7, MYOC, MMP1, TFPI2, CHI3L1, MMP9
GO:0070062	extracellular exosome	1.48988E-05	IL1RN, MMP7, MYOC, PLA2G2A, HP, HBA2, CAPG, MMP9, FCGR3A, SFRP1, DES, CA2, IL1B, APOC1, SPP1, ACP5, CHI3L1, APOD, PI16, FBP1
GO:0031012	extracellular matrix	8.34484E-05	SPON1, SFRP1, MMP7, IBSP, MYOC, MMP1, TFPI2
GO:0031838	haptoglobin-hemoglobin complex	0.009841369	HP, HBA2
GO:0048471	perinuclear region of cytoplasm	0.017958995	CX3CR1, PLA2G2A, SPP1, HMOX1, CHI3L1, APOD
GO:0031988	membrane-bounded vesicle	0.034032333	IBSP, SPP1
GO:0071682	endocytic vesicle lumen	0.038800705	HP, HBA2
GO:0005783	endoplasmic reticulum	0.052251773	MYOC, APOC1, PLA2G2A, HMOX1, CHI3L1, APOD

Table 5 GO annotation Molecular Function

Term	Pathway	PValue	Genes
GO:0004222	metalloendopeptidase activity	0.000159247	MMP12, MMP7, MMP1, ADAM8, MMP9
GO:0008009	chemokine activity	0.000226706	CCL4, CCL3, CCL18, CXCL14
GO:0004252	serine-type endopeptidase activity	0.000363433	MMP12, MMP7, MMP1, HP, ADAM8, MMP9
GO:0004175	endopeptidase activity	0.007603833	MMP12, MMP1, MMP9
GO:0005125	cytokine activity	0.008882175	IL1RN, IL1B, CCL4, SPP1
GO:0031726	CCR1 chemokine receptor binding	0.016880964	CCL4, CCL3
GO:0031730	CCR5 chemokine receptor binding	0.019269721	CCL4, CCL3
GO:0005149	interleukin-1 receptor binding	0.031128822	IL1RN, IL1B
GO:0042802	identical protein binding	0.033983341	SFRP1, DES, CCL4, CCL3, FBP1, MMP9
GO:0005109	frizzled binding	0.083902905	SFRP1, MYOC

Figures

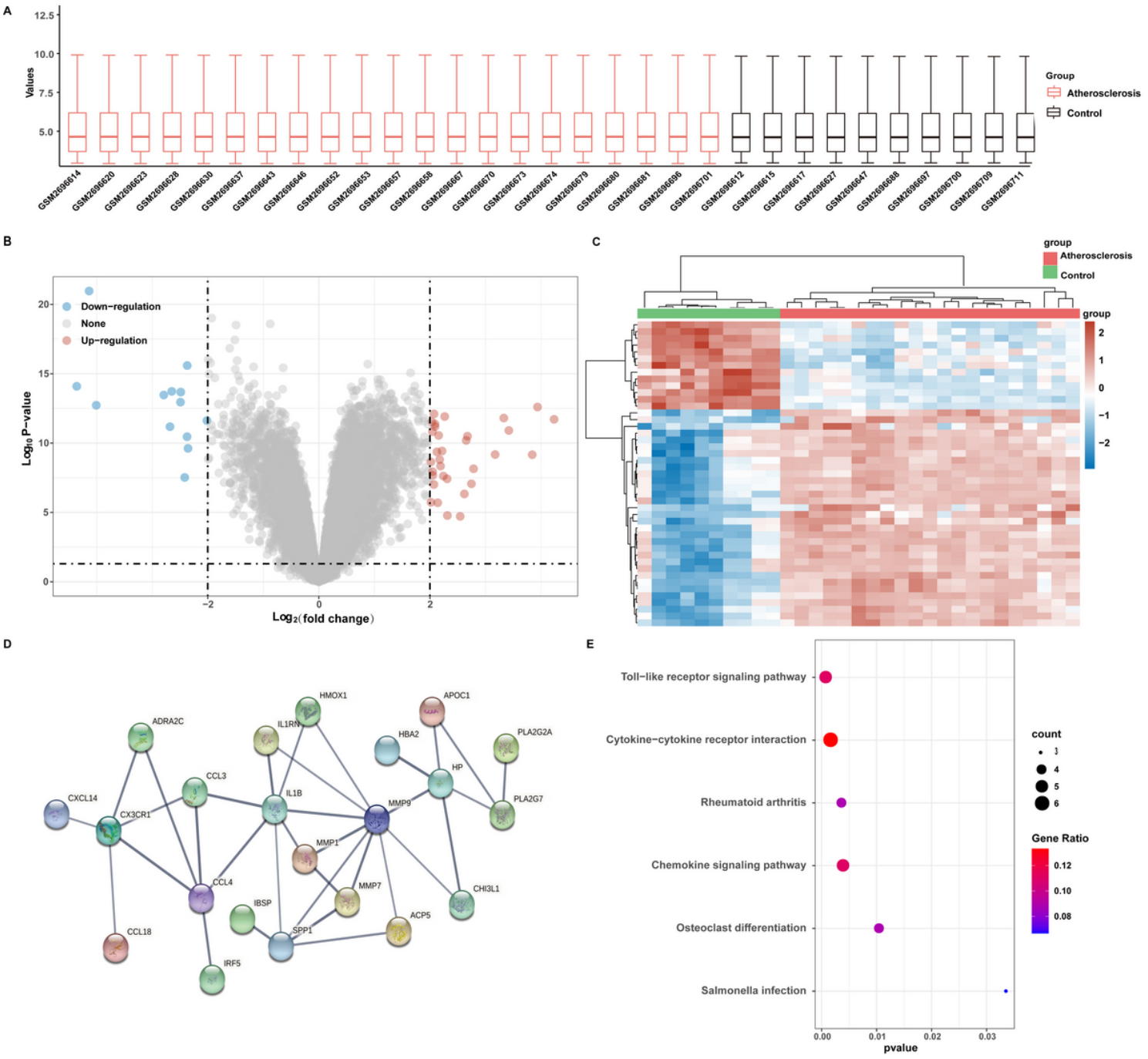

Figure 1

Genes detected according to the DEGs A showed the expression level of each sample from the perspective of the overall dispersion of expression. B showed volcano plot of DEGs (p-value ≤ 0.05 and |log2|≥2). C showed clustered heat map. D showed the interrelationships between proteins. E showed the enrichment of signal pathways and gene expression levels in DEG.

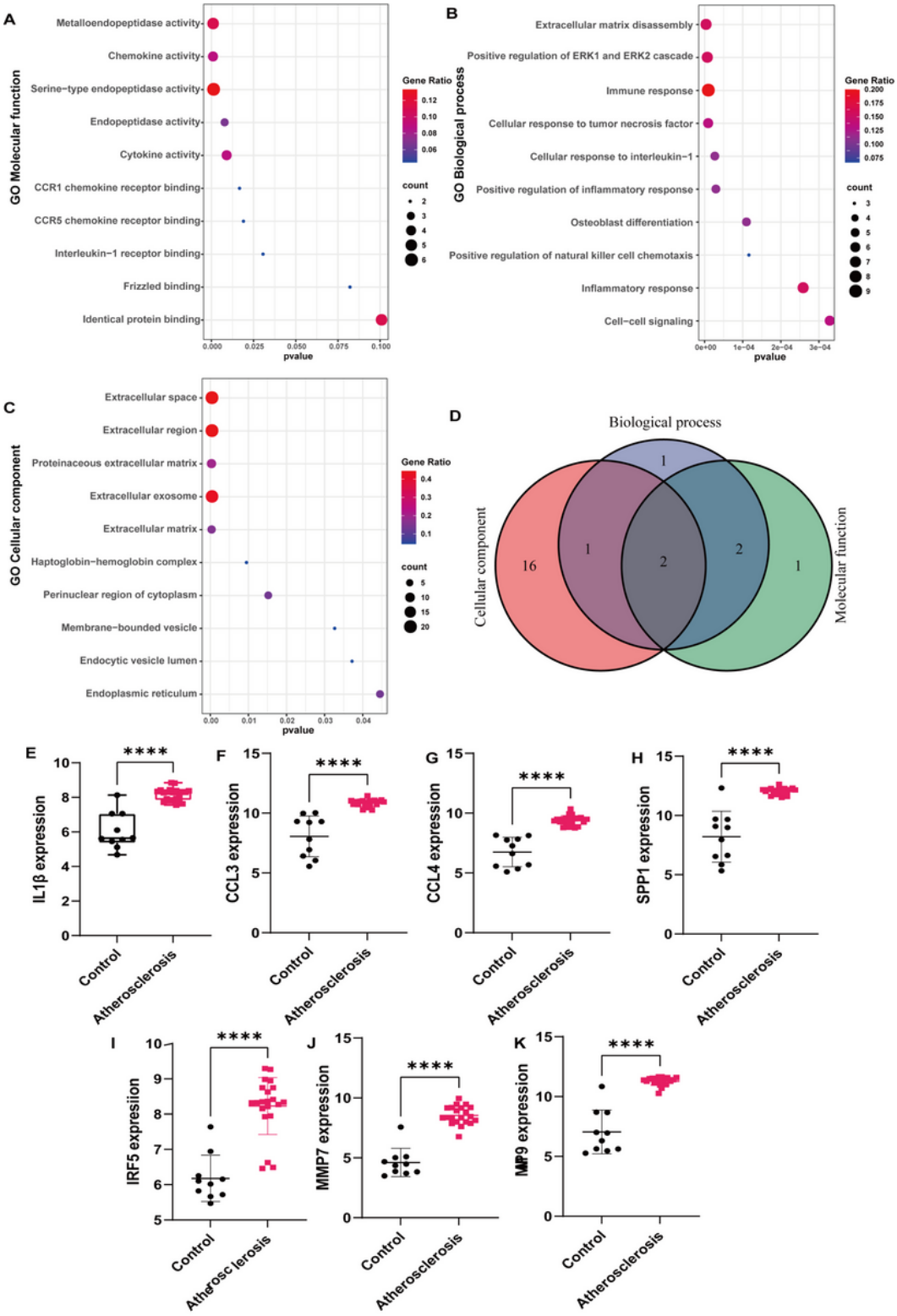

Figure 2

Function Enrichment Analysis of DEG A, B, C showed GO annotation, including Biological Process, Cellular Component, and Molecular Function. D was a Venn diagram showed 2 genes (MMP7 and MMP9) involved in 3 vital GO annotation. E-K showed that the expressions of IL1β, CCL4, SPP1, CCL3, IRF5、MMP7, and MMP9 in Control and Atherosclerosis groups.

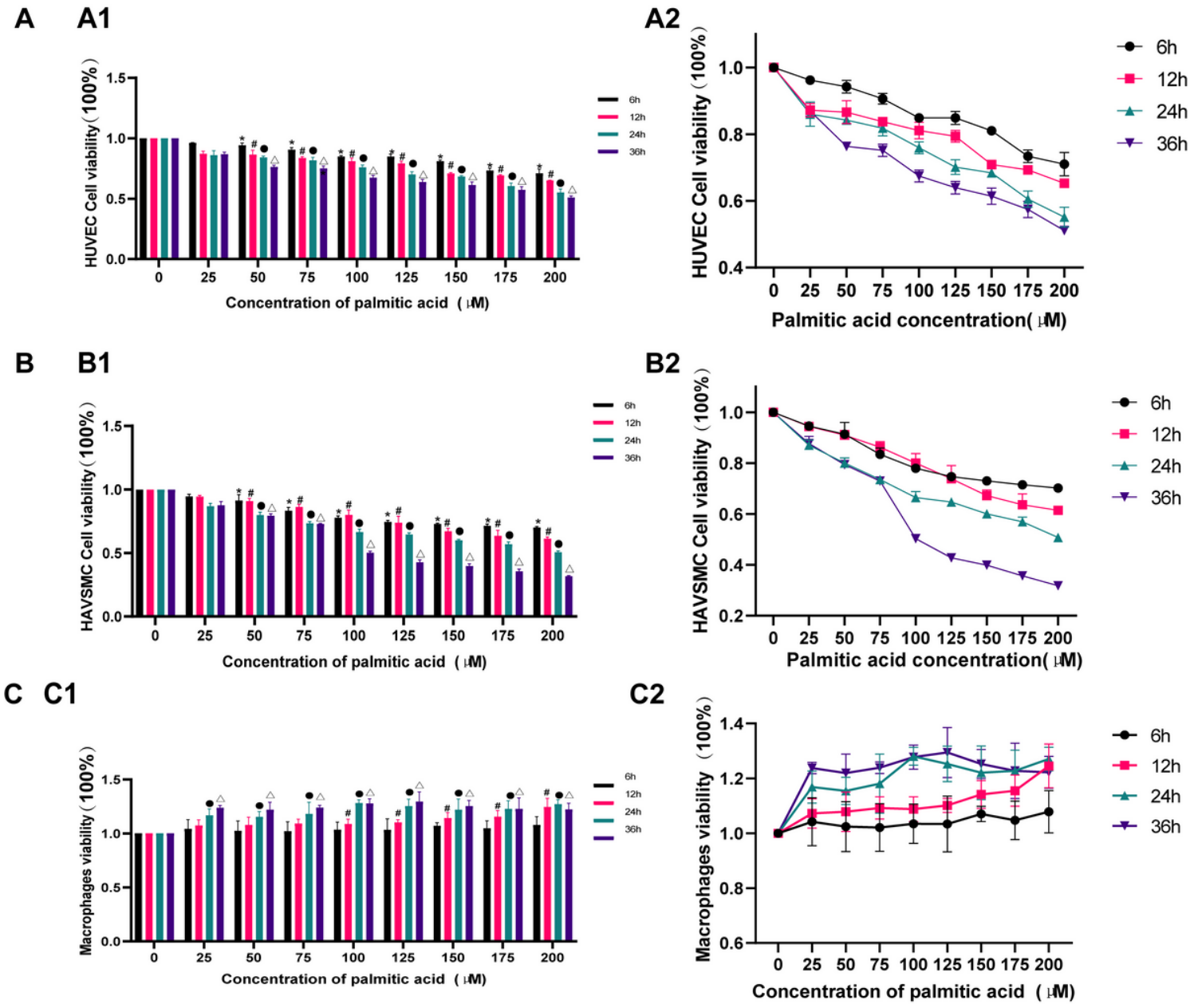

Figure 3

Palmitic acid affected cell viabilities A, B, C showed the effect of palmitic acid on HUVEC, HAVSMC and THP-1 induced macrophages cells viability. * ,#, ●, △ compared with the 0 concentration at 6h, 12h, 24h, 36h individually.

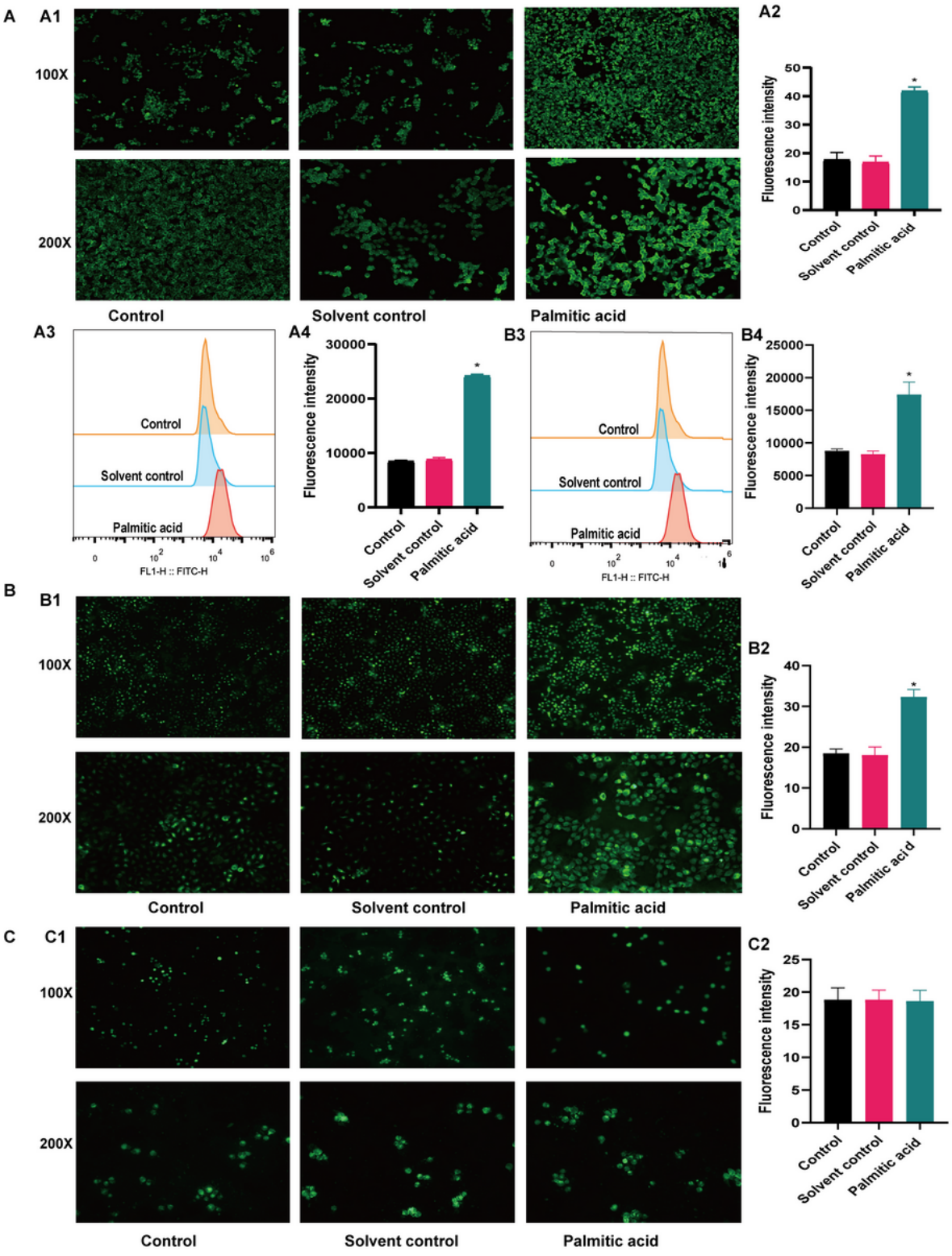

Figure 4

Palmitic acid made cells produce ROS A showed Palmitic acid stimulation for 24 h increased ROS levels of HAVSMC cells (A1 showed ROS fluorescence, A3 showed flow cytometry data, and A2 and A4 show the results of statistical analysis; $p<0.05$). B showed palmitic acid caused the increasing intracellular ROS levels(B1 showed ROS fluorescence, B3 showed flow cytometry data, and B2 and B4 showed the results of statistical analysis; $p<0.05$). C showed palmitic acid and cannot palmitic acid and solvent incubation

cannot change the ROS levels of THP-1 induced macrophages (C1 showed fluorescence, and C2 showed the results of statistical analysis; p<0.05). * compared with the control group.

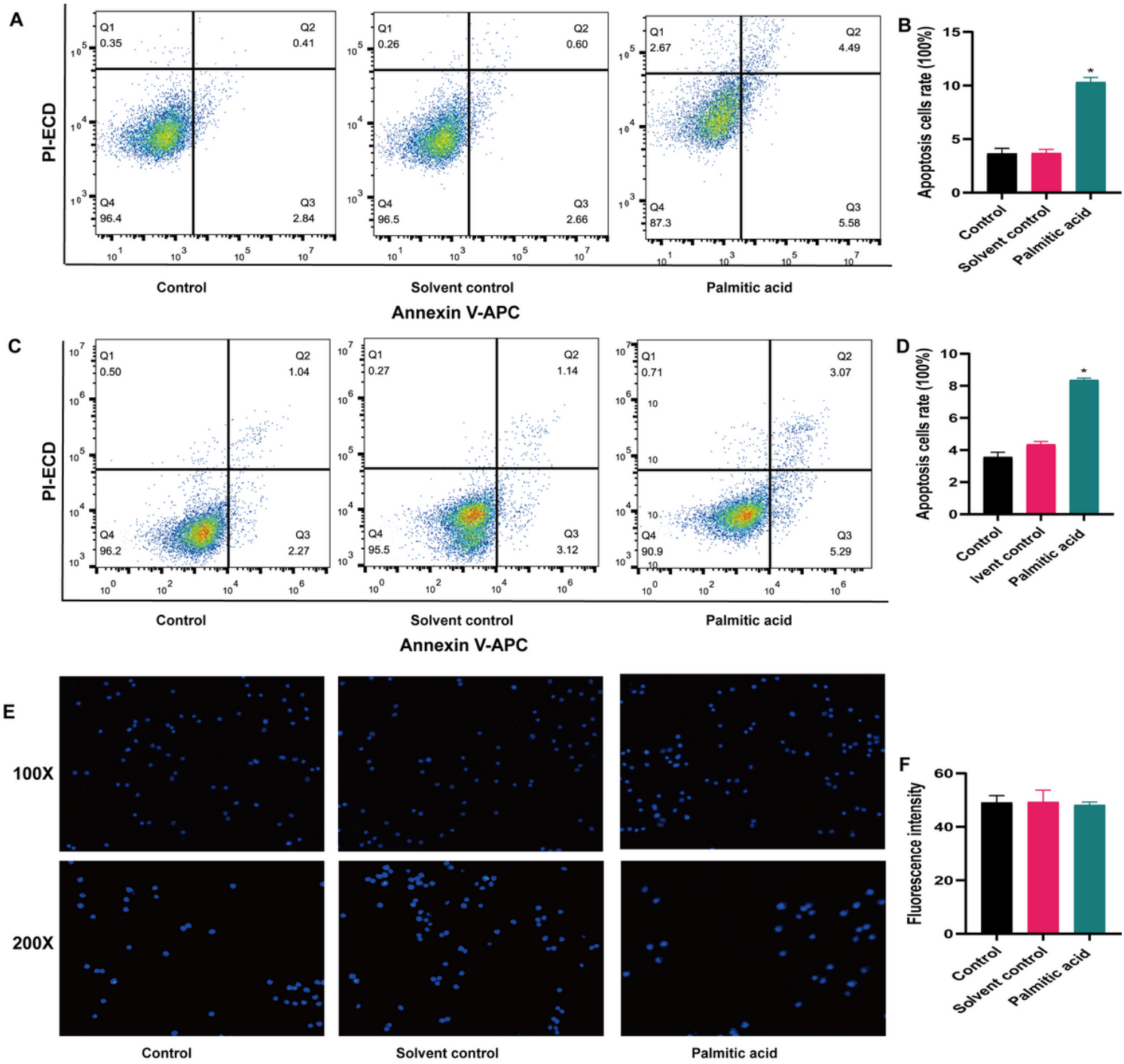

Figure 5

Palmitic acid affected cell apoptosis rates Palmitic acid can lead to HUVEC and HAVSMC cells apoptosis(A,B,C,D, p<0.05). Palmitic acid cannot affect the nucleus morphology of THP-1 induced macrophages. * compared with the control group.

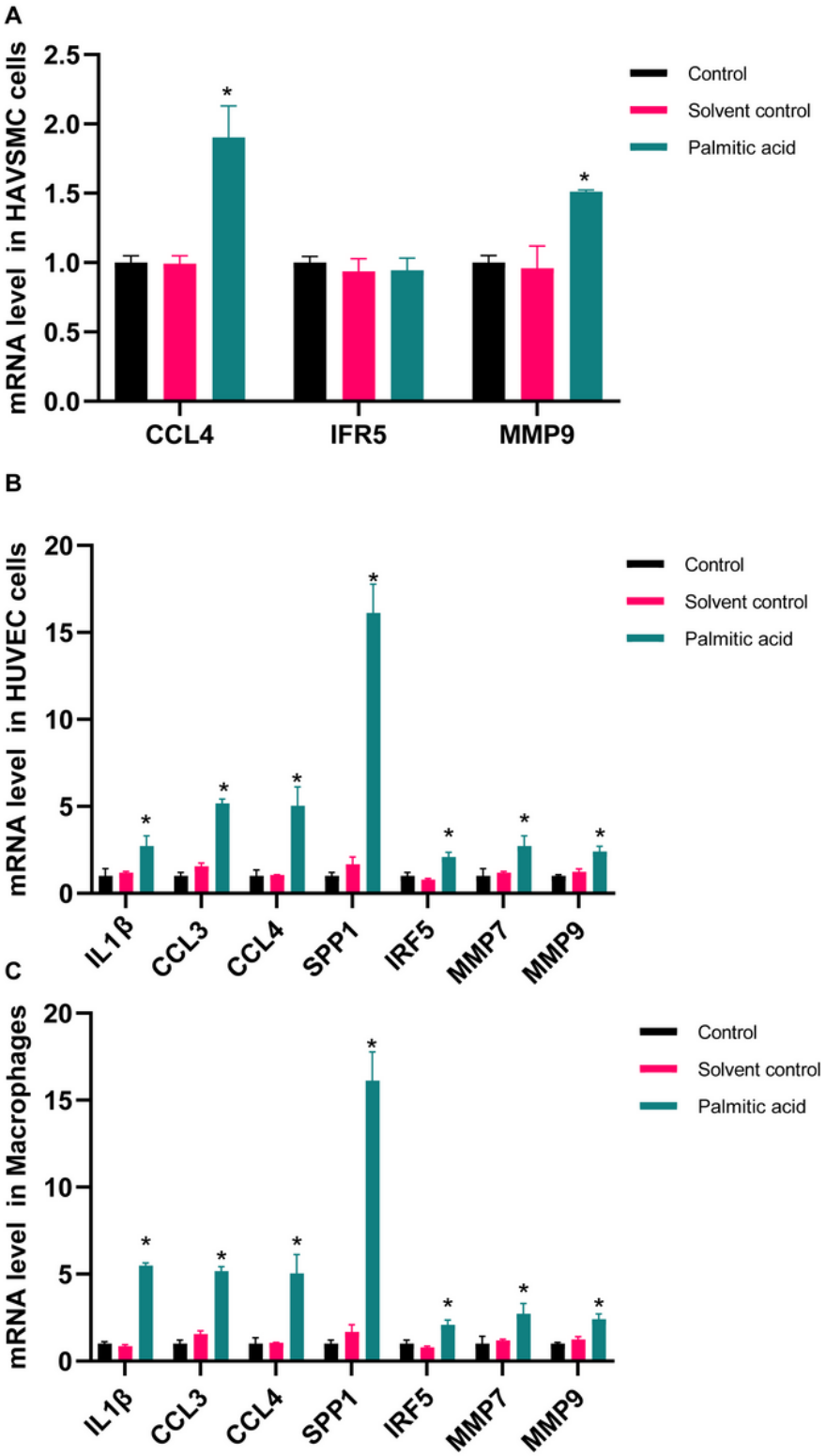

Figure 6

mRNA levels of IL1β, CCL4, SPP1, CCL3, IRF5、MMP7, and MMP9 Palmitic acid increased the levels of IL1β, CCL4, SPP1, CCL3, IRF5、MMP7, and MMP9 both in THP-1 induced macrophages or HUVEC cells(B,C, $p<0.05$). Palmitic acid increased the levels of CCL4 and MMP9(A, $p<0.05$), while the expression level of IRF5 has hardly changed. * compared with the control group.

Supplementary Files

This is a list of supplementary files associated with this preprint. Click to download.

- Supplementarymaterials.xlsx